

# A Novel Chicken Chorioallantoic Membrane Image Vessel Detection Detector Based on Statistic Color Distribution

Chin-Chen Chang\*

Department of Information Engineering and Computer Science  
Feng Chia University  
No. 100, Wen-Hwa Rd., Taichung, Taiwan, 40724, R.O.C.  
Department of Computer Science and Information Engineering  
Asia University  
No. 500, Lioufeng Rd., Wufeng, Taichung, Taiwan, 41354, R.O.C.  
\*Corresponding author  
alan3c@gmail.com

Pei-Yan Pai

Department of Compute Science  
National Tsing-Hua University  
No. 101, Sec. 2, Kuang-Fu Rd., Hsinchu, Taiwan, 30013, R.O.C.  
d938338@oz.nthu.edu.tw

Meng-Hsiun Tsai

Department of Management Information Systems  
National Chung Hsing University  
No. 250, Kuo Kuang Rd., Taichung, Taiwan, 40227, R.O.C.  
mht@nchu.edu.tw

Chia-Ming Liu

Department of Management Information Systems  
National Chung Hsing University  
No. 250, Kuo Kuang Rd., Taichung, Taiwan, 40227, R.O.C.  
ykchan@nchu.edu.tw

Received February, 2013; revised May, 2013

---

**ABSTRACT.** *This paper proposes an automated method to detect the blood vessels on a chicken chorioallantoic membrane image, and computes the BCD of the image based on the extracted blood vessels. It is helpful to enhance the effect of medication in treating or inhibiting cancer. This method first employs Canny edge detector to find out the possible edge pixels of the blood vessel. Next, vessels can be detected by means of the linear formula originated from genetic algorithm. Experimental results show that it is able to recognize almost vessels and BCD error ratio between 2.4% and 3.4%.*

**Keywords:** Chicken chorioallantoic membrane image; Canny edge detector; Genetic algorithm; Box-counting dimension; Vessel segmentation

---

1. **Introduction.** In human beings, blood vessels play a very important role through which nutrient and oxygen can be transported to each organ for proper working. With growth and development of new organizations, blood vessels provide them with necessary nutrient [7]. Thus, wound recovery, tissue repair, reproduction, growth and development need to generate new blood vessels [7]. Production of new blood vessels from original ones is called angiogenesis [7].

Aside from general growth processing to urge angiogenesis, according to clinical experiments, some diseases, such as diabetes, heart vessel disorder, macular retina, and cancer, could cause excessive or inadequate angiogenesis [3, 10]. In order to keep alive, tumorous cells will trigger rapid growth and extension of blood vessels to acquire more nutrient and spread them to other normal organs via vessels [7, 9].

In 1971, Folkman proposed an angiogenesis theory [6] explaining that the growth, degeneration, and metastasis of tumorous cells are closely linked to angiogenesis. With generation of tumors, tumorous cells themselves or organizations around them will ooze a kind of substance to urge angiogenesis by which to obtain more nutrient and oxygen and to metabolize waste material. On the contrary, if we stop abnormal angiogenesis so as to prevent tumorous cells from acquiring adequate nutrient, they will wither and then die [6, 7]. In recent years, the research focused on control of angiogenesis has been done by not a few scholars who presented Anti-angiogenesis treatments [7, 14] in which some medicine is used to suppress activation of abnormal angiogenesis such that tumorous cells can not obtain nutrient and gradually die.

Among new medical researches concentrated on angiogenesis resulted from tumors, Chicken Chorioallantoic Membrane assay (abbreviated to *CAM*), using chicken chorioallantoic membrane formed by rapid vessel generation and without metabolic ability, is a semi in vivo inner experiment to examine the influence level of its vascular generation against some medicine. Through the experiment, the process of angiogenesis triggered by tumors can be simulated. In the so-called “chicken chorioallantoic membrane proliferation assay,” angiogenesis during the first stage after being fertilized is very similar to that urged by tumors. Both are so active that they are suitable for simulating angiogenesis process caused by tumors. Nowadays, there are many clinical medicines used to suppress angiogenesis, e.g. Suramin adopted to restrain combination of its receptors and bFGF for the purpose of control the medicine to urge angiogenesis.

Clinically, there are a lot of meaningful features, such as, color, tube diameter, flex ratio, and distribution density. In the thesis, we use the density of vascular distribution as the property for analysis. Due to a fractal structure shown in vascular distribution, fractal analysis is applied to analyze the density of vascular distribution. By putting vascular pictures into a grid with fixed size, calculate the number of sub-grids through which blood vessels pass, and then use box-counting dimension (*BCD*) [13] to analyze the density of vascular distribution.

The definition of *BCD* follows

$$BCD = \frac{\log N(E)}{\log(\frac{1}{E})}.$$

For the example as shown in FIGURE 1 where there is a grid of sub-grids with edge size  $E = 1/5$ , and the number of sub-grids through blood vessels pass  $N(E) = 11$ , we can calculate  $BCD = 1.49$ . The less the value of *BCD* is, the less the density of vascular distribution will be. Accordingly, *BCD* is very suitable for analysis of density of vascular distribution.

By means of calculation of *BCD*, we can analyze if some medicine is effective or not in suppressing or stimulating angiogenesis. The advantage of *CAM* is its low cost, no

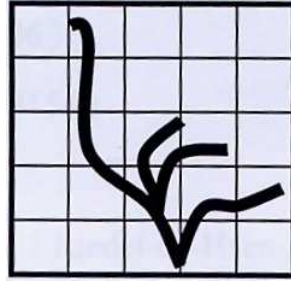


FIGURE 1. Fractal analysis grid

vivisection, direct examination of vascular distribution, and follow-up state tracing of angiogenesis. However, it is very time-consuming to calculate by hand  $BCD$  for a chicken chorioallantoic membrane image. So, it is worthy of investigation and research to develop an automatic system to calculate automatically  $BCD$  in aid of biomedical workers.

Generally, border lines exist in both sides of blood vessels for a chicken chorioallantoic membrane image. In the paper, we first use canny edge detector to detect vascular border lines. Next, according to the difference between blood vessels and others found by means of the statistics of color distribution, determine if the pixels around vascular border lines are vascular pixels. Finally, calculate automatically  $BCD$  for the chicken chorioallantoic membrane image in order to help biomedical workers do the follow-up working.

**2. Blood Vessel Detection Methodology.** A full-color chicken chorioallantoic membrane image is composed of RGB. For the purpose of analyzing the difference of color distribution between blood vessels and others, we requested experts to randomly extract R, G and B components of 400 vessel and 400 non-vessel pixels selected by hand from several chicken chorioallantoic membrane images. TABLE 1 displays the distribution of such pixels on various components in which VC stands for the number of vessel pixels in some area whereas NC that of non-vessel pixels. OP, which is an overlap probability of vessel parts and non-vessel ones in some area, is calculated by subtracting the smallest value from the largest value and then dividing the result by the number of both vessel and non-vessel parts in the area while the average of overlap probabilities for components is indicated by Average whose value, smaller, means its better ability to distinguish vessel from non-vessel parts.

According to TABLE 1, G component is most suitable for discriminating between vessel parts and non-vessel ones. This is due to the fact that the standard deviation around vascular edge varies greater in a grey image than that of background in the image does. Thus, we also use the standard deviation of G component as one of characteristics. In addition to analyze the difference of RGB against vessel and non-vessel parts, we transform RGB into YCrCb to find with its chromatism the difference between vessel and non-vessel parts, as shown in TABLE 1 showing the value of Y component is easily affected by shooting light although it can differentiate vessel parts and non-vessel ones along with no ability for Cb component to judge between shadow and vessels and better capability for Cr component to separate vessel parts from others.

In general, there are side lines in both sides of vessels, so we can use Edge detector to find both side lines in order to position the vessels. Because color values of vessels in a grey image tend to black and the standard deviation around edge varies greater than that of background, the above features can be used to determine if the pixels around vascular edge lines are vascular.

TABLE 1. Statistics color distribution

	R			G			B			Y		
	VC	NC	OP	VC	NC	OP	VC	NC	OP	VC	NC	OP
201~255	42	170	0.25	0	0	0	0	34	0	0	55	0
161~200	160	102	0.64	0	70	0	0	37	0	2	163	0.01
121~160	174	96	0.55	15	148	0.1	0	32	0	33	110	0.3
81~120	24	28	0.86	161	64	0.4	1	129	0.01	274	54	0.2
41~80	0	4	0	231	18	0.08	234	143	0.6	89	17	0.19
0~40	0	0	0	38	1	0.03	165	25	0.16	2	1	0.5
Average	-	-	0.46	-	-	0.122	-	-	0.154	-	-	0.24

	Cr				Cb				Standdeviation		
	VC	NC	OP		VC	NC	OP		VC	NC	OP
61~85	79	0	0	21~40	0	0	0	15~60	36	7	0.19
46~60	166	0	0	1~20	0	42	0	13~15	31	3	0.1
31~45	87	43	0.49	-19~0	31	80	0.39	10~12	31	2	0.06
16~30	53	208	0.25	-39~-20	327	90	0.28	7~9	71	4	0.06
1~15	15	88	0.17	-59~-40	40	155	0.28	4~6	125	23	0.18
-30~0	0	61	0	-80~-60	2	33	0.06	0~3	106	361	0.29
Average	-	-	0.182	Average	-	-	0.202	Average	-	-	0.176

According to the features mentioned above, the proposed approach falls into three steps. The first step is to extract G color component from a full-color chicken chorioallantoic membrane image, to combine the component into a grey image and, to detect both sides of vessels, called hard edges, by means of Canny edge detector. Next, we take advantage of genetic algorithm with use of G component, its standard deviation, and Cr as features to find the difference between vessel parts and others for the purpose of determining if a pixel in the grey image is a vessel candidate. Finally, use the above characteristics in the second step to decide if the pixels around hard edges are vessel pixels. We call the proposed method statistic color distribution based vessel detector (*SCDVD*). In the following, we shall introduce the mechanism in detail.

In the first phase, *SCDVD* is to extract G component from a full-color chicken chorioallantoic membrane image, and combine the component into a grey image, called G gray-level image. Generally, noise could happen in an image as a result of photography, scanning, and transferring. However, the noise would make the extraction of needed information difficult. We, therefore, adopt a  $3 \times 3$  medium filter [5] to remove the noise in G gray-level image.

Canny edge detector [1, 2] is an approach, which is widely used and proved effective in detection of edges. In this paper, we apply the algorithm to the detection of both sides of vessels in a G gray-level image. Canny edge detector firstly capitalizes Gaussian filter to remove the noise in the image and then adopts horizontal and vertical operators in Sobel method to find edge intensities of pixel, which accordingly is applied to analysis of edge angle for edge point. Edge angle is calculated by  $\tan^{-1}E_y/E_x$ , where  $E_x$  and  $E_y$  are the vertical and the horizontal edge intensities in the image, respectively. After that, non-maximum suppression is applied to trace the edge (set to be 1) and suppress the pixels which are not located at edges (set to be 0).

Determining if a pixel is an edge point by setting single threshold is very likely to make the threshold setting excessively high such that several true edges, namely vascular edges, may be ignored; conversely, to make the threshold setting excessively low may result in

several false edges, namely non-vessel edges. As a result, we adopt two thresholds as inputs to Canny edge detector: a high threshold  $T_h$  and a low threshold  $T_l$ . Next, scan in order each pixel edge intensity in the image, and set the pixel to be a hard edge point while its edge intensity is greater than or equal to  $T_h$ . At the same time, set the hard edge point to be a center of a  $3 \times 3$  mask to examine if its eight neighbor pixel edge intensities are less than  $T_h$  and greater than or equal to  $T_l$ . If the condition is true, its neighbor pixels are treated as hard edge points; otherwise, as non-edge pixels. Afterwards, mark each hard edge pixel and the other by bits 1 and 0, respectively. These 0's and 1's result in a bi-level image. A bi-level image, we call edge image  $I_e$ , resulted from G grey-level image via Canny edge detector is depicted in FIGURE 2 in which  $T_l$  and  $T_h$  are set, respectively, 0.05 and 0.015.

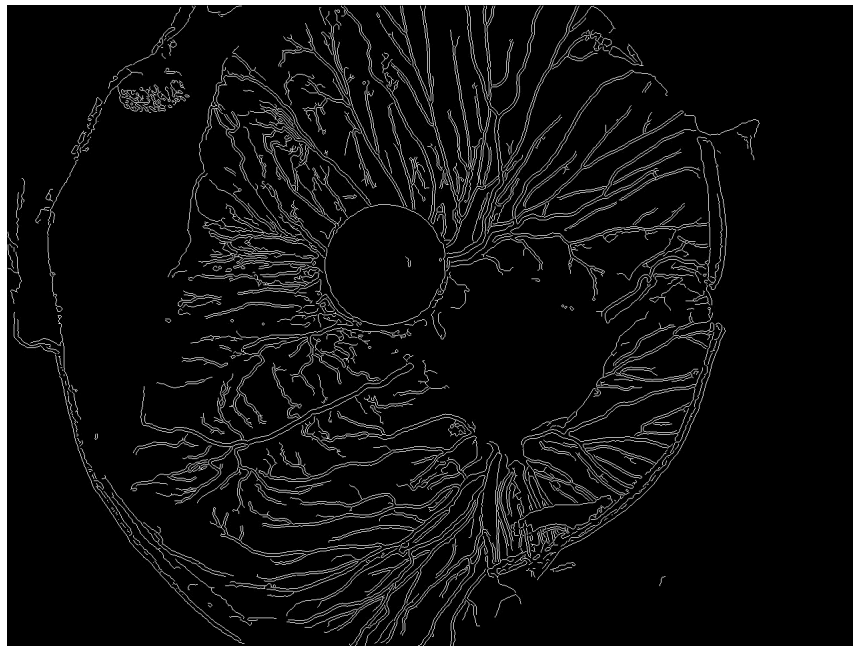
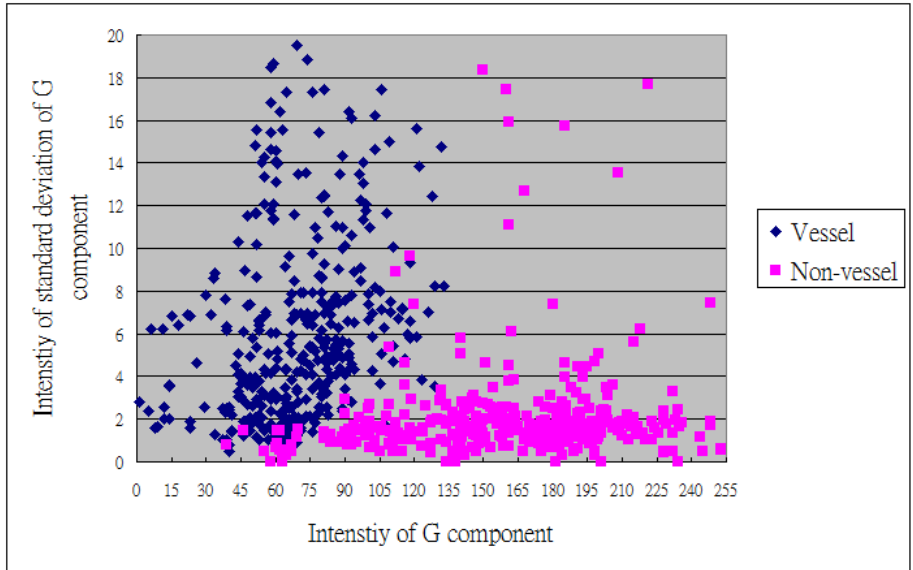


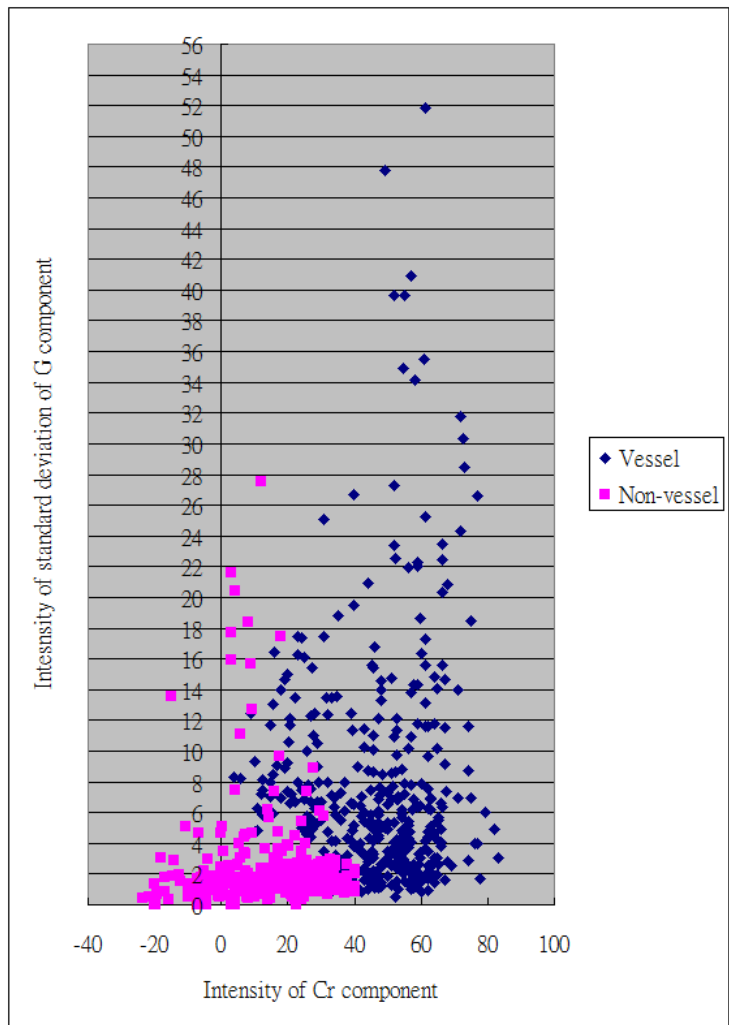
FIGURE 2. An edge image through Canny edge detector processing

Canny edge detector is to use the gradient among pixels to detect edge points, so vascular edges can be found. However, non-vessel edges, such as, eggshell, eggshell membrane etc., would be found because Canny edge detector only considers the size of edge intensity. Because vascular color is different from eggshell and eggshell membrane colors, we adopt pixel color to remove non-vessel parts from edge points acquired by Canny edge detector. Additionally, vascular color in G grey-level image is generally darker and the standard deviation around edges varies greatly, we utilize the standard deviation combined with two features, color and hue, to detect the possible vascular pixels.

According to the analysis in TABLE 1, R component can't be used to find the relationship between vessel pixel and non-vessel one. B and Cb components can be applied to distinguishing vessel pixel from the other, but to judge the difference between vessels and darker (or shadow) parts in the image. Y component is not considered due to being easily affected by shooting light. G component, Cr component, and standard deviation of G component are all suitable for differentiating vessels and others. However, it is not sufficient by using one of the three characteristics to find vascular pixels. Thus, we combine G component and Cr component with standard deviation of G component. FIGURE 3 shows the resulted relationship distribution of vessel pixels and non-vessel ones.



(a) The relationship of vessel and non-vessel pixels of G combined with standard deviation of G



(b) The relationship of vessel and non-vessel pixels of Cr combined with standard deviation of G

FIGURE 3. The relationship of vessel and non-vessel pixels of combined components

Through the analysis diagram shown in FIGURE 3, we can find each optimal straight line in these histograms to differentiate vessel pixels from others as far as possible, as depicted in dotted line. The linear formula is defined as  $y = ax + b$ , where  $a$  stands for the slope of the straight line and  $b$  is the intercept. With different  $a$  and  $b$ , varies the correctness of discrimination between vessel and others. Then we will use genetic algorithm to obtain the most suitable values of  $a$  and  $b$ .

The spirit of genetic algorithm [12] is to express a solution to a problem by genetic patterns in chromosome, constantly transform gene, and reorganize the problem in order to reproduce superior descendants. In other words, each evolution takes it further toward the optimal solution such that the approximately optimal solution can be found in the long run. Chromosome encoding is the major job in genetic algorithm. Among encoders, binary encoder is most widely employed. The encoder converts variables into a binary string, a so-called solution, consisting of 0's and 1's in which each variable is mapped to a substring.

The *SCDVD* makes use of a binary string comprising  $M + K$  bits to represent a chromosome  $Ch$  in which the first  $M$  bits and the remaining  $K$  bits are used to describe the values of  $a$  and  $b$ , respectively. The value of  $a$  is the sum of a base ( $Base_a$ ) and  $p_{r_1}$  multiplied by the number of bit 1's from the first  $M$  bits in  $Ch$  while the value of  $b$  sums a base ( $Base_b$ ) and  $p_{r_2}$  multiplied by the number of bit 1's of from the remaining  $K$  bits in  $Ch$ , where  $p_{r_1}$  (or  $p_{r_2}$ ) is the increments of  $a$  (or  $b$ ).

Given a chromosome, we can calculate the values of  $a$  and  $b$ . Then, the *SCDVD* takes advantage of the two values to find the optimal linear formula whereby to detect vessel pixels from 800 pixels in which 400 pixels are known as vascular and the others as non-vessel. The correctness of discrimination between vessel and others is used as the chromosome fitness whose definition is as follows:

$$Fitness = \frac{A - G_w}{A} \times 100\% \quad (1)$$

where  $A$  is a given total number of vessel and non-vessel pixels and  $G_w$  is the number of misreckoned pixels caused by the linear formula. In the thesis,  $A$  is 800 while both vessel pixels and non-vessels are 400. A larger fitness indicates a stronger fitness of the chromosome.

While running the genetic algorithm, the *SCDVD* first generates by a random number generator  $T$  random chromosomes. Afterwards, the most competent generation survives after continuous evolution among which each generation goes through three steps: mutation, crossover, and selection. In each evolution,  $T$  chromosomes with optimal fitness values are kept until their fitness values are similar to one another.

In mutation step, for each one among  $T$  reserved chromosomes, the *SCDVD* uses a random number generator to randomly choose a bit  $b_1$  and a bit  $b_2$ , respectively from the first  $M$  bits and the remaining  $K$  bits of each reserved chromosome, respectively. Also,  $b_1$  and  $b_2$  are replaced respectively by  $\neg b_1$  and  $\neg b_2$  to generate new  $T$  chromosomes, where  $\neg$  means the operator of "not".

In crossover step following the above, the *SCDVD* similarly uses a random number generator to randomly designate two chromosomes as a pair among  $T$  reserved chromosomes in each evolution such that  $T'$  pairs of chromosomes are determined. Let  $Ch[i..j]$  be the values from the  $i$ -th bit to the  $j$ -th bit in a chromosome  $Ch$ . For each pair of chromosomes  $Ch_1$  and  $Ch_2$ , the *SCDVD* concatenates orderly  $Ch_1[1..\lfloor M/2 \rfloor]$ ,  $Ch_2[(\lfloor M/2 \rfloor + 1)..M]$ ,  $Ch_1[(M + 1)..(M + \lfloor K/2 \rfloor)]$ , and  $Ch_2[(M + \lfloor M/2 \rfloor + 1)..(M + K)]$  into one new chromosome. Likely,  $Ch_2[1..\lfloor M/2 \rfloor]$ ,  $Ch_1[(\lfloor M/2 \rfloor + 1)..M]$ ,  $Ch_2[(M + 1)..(M + \lfloor K/2 \rfloor)]$ , and  $Ch_1[(M + \lfloor M/2 \rfloor + 1)..(M + K)]$  are in order conjoined into another new chromosome.

Now, there are  $T$  reserved chromosomes,  $T$  chromosomes generated in mutation step, and  $T'$  chromosomes produced in crossover step. In selection step,  $a$ 's and  $b$ 's derived from these chromosomes are given to Equation (1) to calculate their fitness. Finally, only  $T$  chromosomes with the highest correctness are reserved into next evolution process until the fitness values of the reserved  $T$  chromosomes are extremely similar.

The parameters given to genetic algorithm are set as  $M = K = 20$ ,  $N = N' = 500$ . On calculating the linear formula for G combined with standard deviation of G,  $Base_a = Base_b = 0$ ,  $p_{r_1} = 0.015$ ,  $p_{r_2} = -0.5$ . If there are a number  $x_1$  of 1-bits in  $Ch[1..M]$  and a number  $x_2$  of 1-bits in  $Ch[M+1..M+K]$  from each chromosome, then  $a = Base_a + x_1 \times p_{r_1}$  and  $b = Base_b + x_2 \times p_{r_2}$ ; Moreover, we run 8 generations of evolutions in the experiment in support of (1) to obtain fitness for each chromosome. While computing the linear formula for Cr combined with standard deviation of G,  $Base_a = Base_b = 0$ ,  $p_{r_1} = -0.05$ ,  $p_{r_2} = 1$ . The remaining procedures are true of the above.

The follow-up experiments in the paper are also according to the above parameters. Equations (2) and (3) are the optimal linear formula, obtained by genetic algorithm, for G combined with and that for Cr combined with standard deviation of G, respectively.

$$y_{GSd} = 0.075x - 4.5 \text{ for G-standard deviation} \quad (2)$$

$$y_{CrSd} = -0.2x + 9 \text{ for Cr-standard deviation} \quad (3)$$

in which  $x$  is the value of G component in (2) or that of Cr component in (3), and  $y_{GSd}$  and  $y_{CrSd}$  are the standard deviation calculated via (2) and that by (3), respectively.

In the following, we define the distance between Equations (2) and (3) and each pixel in a chicken chorioallantoic membrane image as follows:

$$y'_{GSd} = \begin{cases} y_{GSd}/\overline{y_{GSdT}}, & \text{if } y_{GSd} \geq 0 \\ y_{GSd}/\overline{y_{GSdF}}, & \text{if } y_{GSd} < 0 \end{cases},$$

$$y'_{CrSd} = \begin{cases} y_{CrSd}/\overline{y_{CrSdT}}, & \text{if } y_{CrSd} \geq 0 \\ y_{CrSd}/\overline{y_{CrSdF}}, & \text{if } y_{CrSd} < 0 \end{cases}, \text{ and} \quad (4)$$

$$\text{Distance} = (y - y'_{GSd}) + (y - y'_{CrSd}),$$

where both  $y'_{GSd}$  and  $y'_{CrSd}$  are formalized values.  $\overline{y_{GSdT}}$  and  $\overline{y_{CrSdT}}$  are the average of  $y_{GSd}$  and that of  $y_{CrSd}$ , respectively, in case of  $y_{GSd}$  and  $y_{CrSd} \geq 0$  whereas  $\overline{y_{GSdF}}$  and  $\overline{y_{CrSdF}}$  are those averages in case of  $y_{GSd}$  and  $y_{CrSd} < 0$ . The larger Distance is, the more probably a pixel is vascular; conversely, with the smaller Distance comes with a non-vessel pixel. We divide Distance into 256 levels and use them to construct a gray-scale image, as shown in FIGURE 4. Afterwards, by means of Otsu method [11] along with the histogram of the image, we compute a threshold such that the image can be categorized into two groups in which one group is greater than the threshold, i.e. vessel pixels and the other is less than the threshold, i.e. non-vessel pixels. Moreover, in a group, the difference between elements is the smallest; between groups, the difference of individual elements is the largest. FIGURE 5 shows a predicted bi-level vascular image  $I_c$  with Otsu method transformation, where bit '0' and '1' are respectively a non-vessel pixel and a vessel pixel.

We define a seed pixel as a pixel, which is bit '1' in  $I_c$  and corresponds to a pixel in  $I_c$ . Moreover, the directions vessels pass are classified as: vertical one, horizontal, two diagonal ones (one is from the left top to the right bottom and the other is from the right top to the left bottom).

Detecting vascular pixels of  $SCDVD$  is divided into two stages. The first is from left to right to scan each pixel  $I_c$  and consider it a vascular pixel if it is near seed pixels and its surroundings are for the most part bit '1' in  $I_c$ . In the stage, we can detect those pixels from vessels extending in vertical order and two diagonal ones. The other stage is to scan

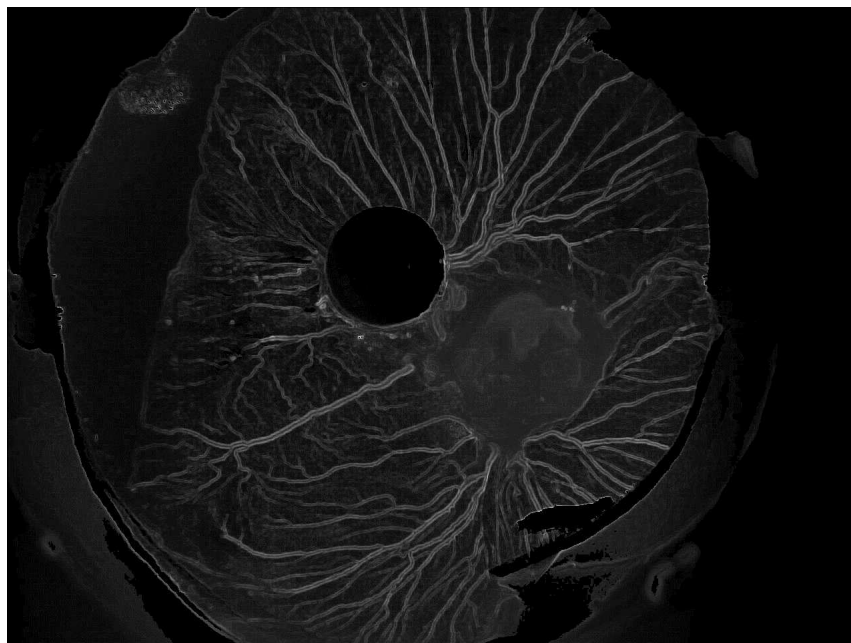


FIGURE 4. A gray-scale image with 256 levels via Distance formalization

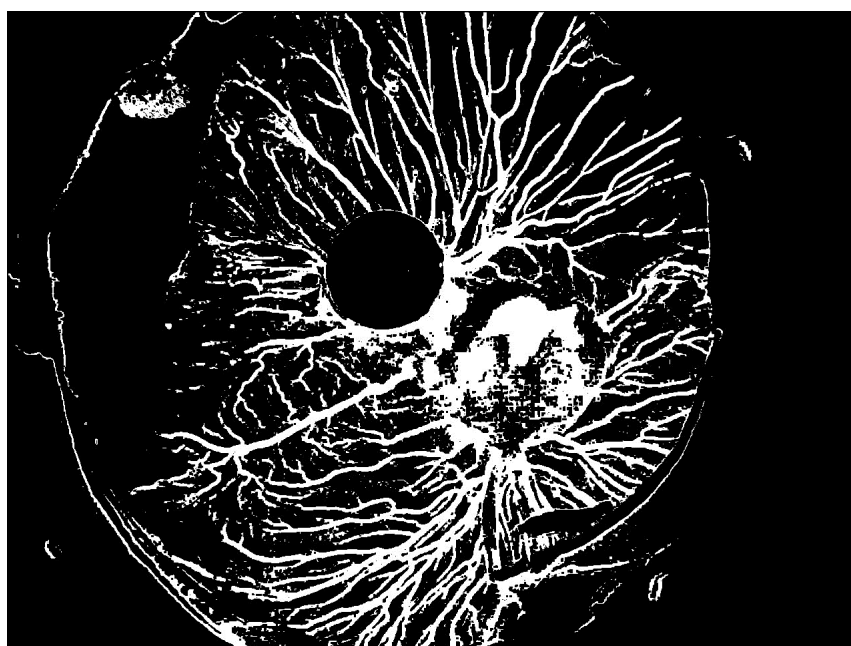


FIGURE 5. A predicted bi-level vascular image

each pixel in  $I_c$  from top to bottom and consider it a vascular pixel by the same way as the first stage. The pixels from vessels extending in horizontal direction can be detected in the stage.

Let  $G(x, y)$  be the current pixel being scanned, where  $(x, y)$  is the position of  $G(x, y)$  located on an image. Because Canny edge detector utilizes the gradient between pixels to detect edge points, great change of the gradient causes a pixel to be regarded as an edge point, but the pixel is actually neither a vascular pixel nor an edge point. However,

a vessel, in general, includes two edge lines, a characteristic, which adopted in the paper for a simple measurement.

In the first stage, if  $G(x, y)$  is a seed pixel and there exists two or more corresponding edge points at 0, 45, or 315 degree, as shown in FIGURE 6(a), we will determine if  $G(x, y+1)$  conforms to the condition to be a vessel pixel. On the contrary, keep finding new seed pixel to start new judgment until the vascular condition is violated. The algorithm for the first stage is presented below. In the second stage, if  $G(x, y)$  is a seed pixel and there exists two or more corresponding edge points at 225, 270, or 315 degree, as shown in FIGURE 6(b), we will determine if  $G(x, y+1)$  conforms to the condition to be a vessel pixel. If the condition is meet, we start from  $G(x+1, y)$  to judge if next pixel is a vessel pixel until the condition is infringed. Conversely, keep finding new seed pixel to start new judgment. The algorithm for the stage is shown below.  $m \times n$  is a small scope around  $G(x, y)$ ;  $\overline{C}_r$ ,  $\overline{C}_l$ ,  $\overline{C}_d$ , and  $\overline{C}_u$  are respectively a small scope to the right of, one to the left of, one on the bottom of, and one on the top of the seed pixel.  $I_c$  is the predicted number of total vessel pixels.  $THR$  is a threshold.  $V$  is the result, a bi-level image in which vessel pixels and non-vessel ones are marked respectively as bit '1' and '0'. FIGURE 7 illustrates the bi-level image  $V$  from FIGURE 6 through the above stages.

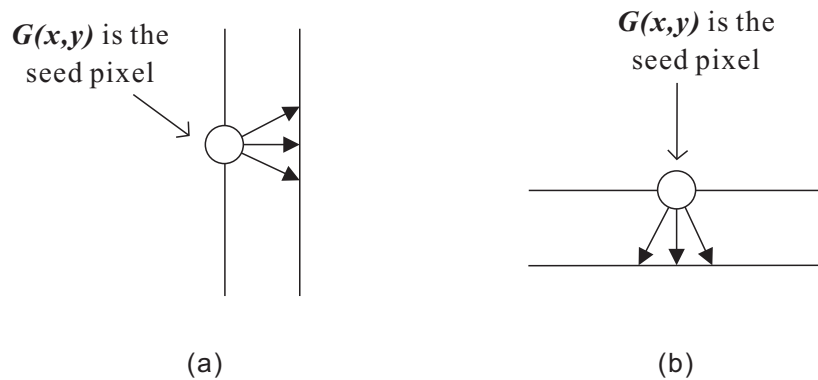


FIGURE 6. (a) Corresponding edge point at 0, 45, or 315 degree (b) Corresponding edge point at 225, 270, and 315 degree

In the above stage, the noise implied by an image would make a few vessels broken, as depicted in the red circle of FIGURE 8. Generally speaking, if a pixel exists in a vessel, it should be a vessel pixel. Thus, if the number of the vessel pixels among the pixels around a black enclosure is greater than a threshold  $T_v(m \times n \times 30\%)$ , then set all pixels in the black enclosure to be vessel pixels.  $V$  through patching holes as mentioned above is shown in FIGURE 9.

In addition to make vessels broken, noise would also cause some non-vessel pixels to be considered vessel pixels, as shown in the red circle of FIGURE 10. On the whole, vessels usually have edge lines, but the pixels mistaken for vessel pixels as a result of noise have no edge lines around them, a feature used by *SCDVD* to remove mistaken vessel pixels.

At first, our method is to scan each pixel in  $V$  from left to right. For each pixel being traversed  $V(x, y)$ , if all pixels of  $V(x, y-1)$  and  $V(x, y+N)$ ;  $V(x, y-1)$  and  $V(x, y+(N-1))$ ;  $V(x, y-1)$  and  $V(x, y+2)$ ;  $V(x, y-1)$  and  $V(x, y+1)$ ;  $V(x, y+1)$  and  $V(x, y-N)$ ;  $V(x, y+1)$  and  $V(x, y-(N+1))$ ;  $V(x, y+1)$  and  $V(x, y-2)$ ; and  $V(x, y+1)$  and  $V(x, y-1)$  are non-vessel pixels and among the regions is no pixel belonging to vascular edge lines, then set all pixels located in the regions to be non-vessel pixels where  $N$  is the diameter of patched holes.

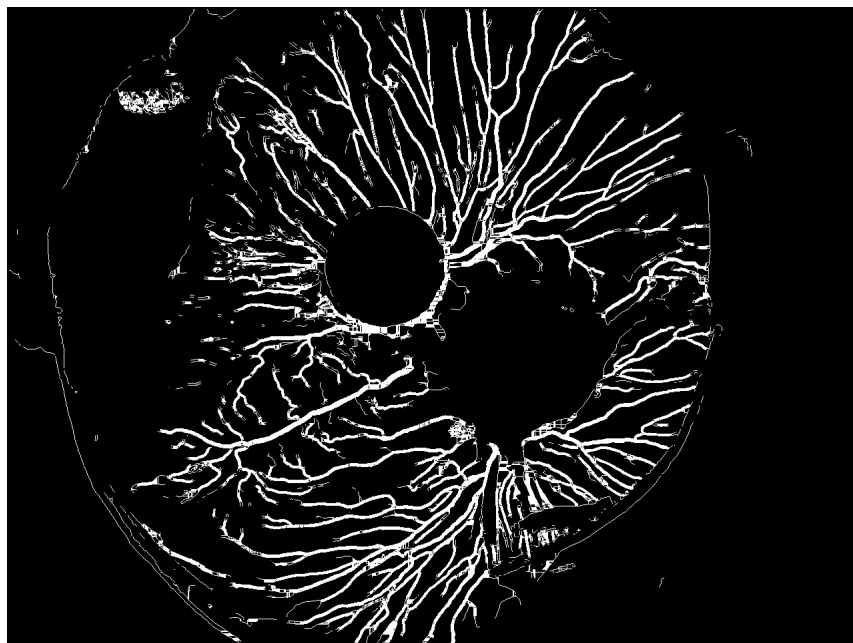


FIGURE 7. Vessel image ( $THR = 5 \times 5 \times 0.25$ )



FIGURE 8. Broken phenomenon in vessels

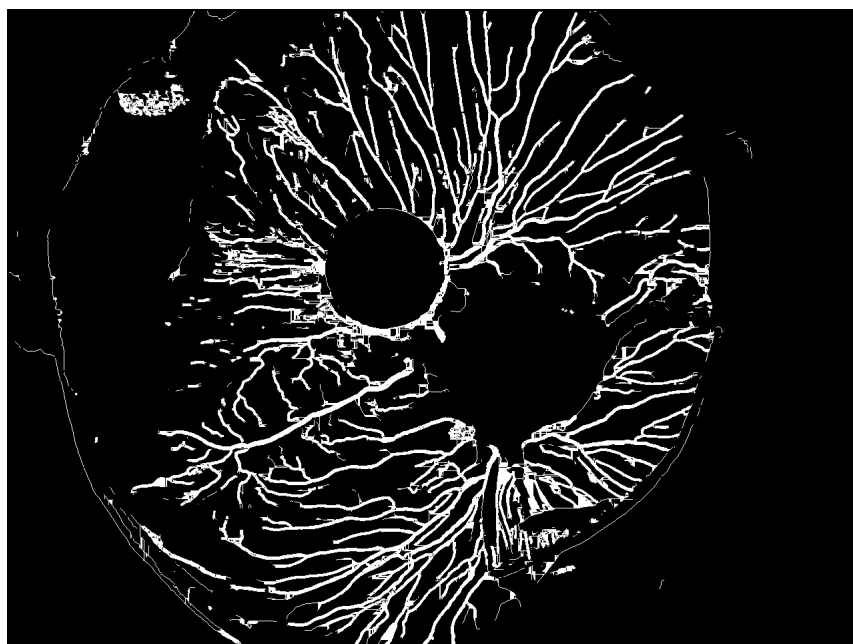


FIGURE 9.  $V$  through patching holes



FIGURE 10. An illustration of mistaken vessel pixels

Similarly, scan every pixel once again in top-down fashion. For each pixel being visited  $V(x, y)$ , if all pixels of  $V(x - 1, y)$  and  $V(x + N, y)$ ;  $V(x - 1, y)$  and  $V(x + (N - 1), y)$ ;  $V(x - 1, y)$  and  $V(x + 2, y)$ ;  $V(x - 1, y)$  and  $V(x + 1, y)$ ;  $V(x + 1, y)$  and  $V(x - N, y)$ ;  $V(x + 1, y)$  and  $V(x - (N - 1), y)$ ;  $V(x + 1, y)$  and  $V(x - 2, y)$ ;  $V(x + 1, y)$  and  $V(x - 1, y)$  are non-vessel pixels and among the regions is no pixel belonging to vascular edge lines, then set all pixels located in the regions of these coordinates to be non-vessel pixels. FIGURE 11 illustrates the result by running the above procedures on FIGURE 10.

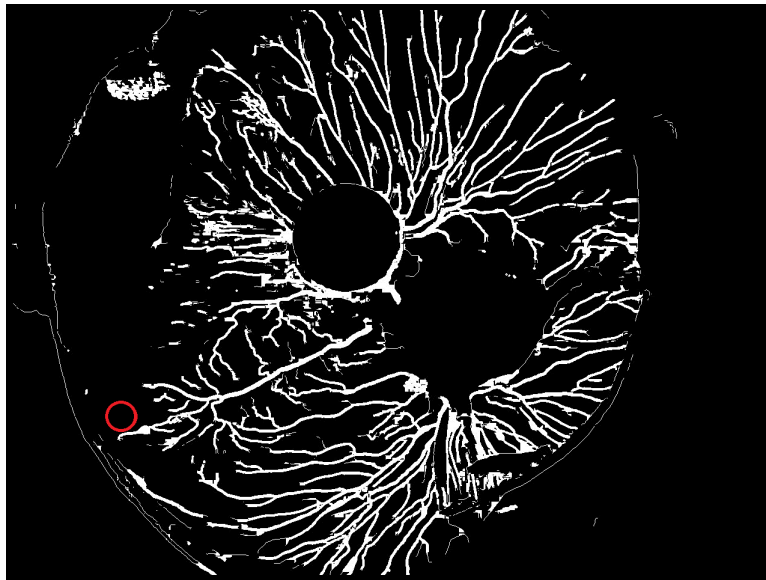


FIGURE 11.  $V$  with removal of mistaken pixels

The goal of Canny edge detector is to find the edge parts in an image. Therefore, non-vessel edges, such as eggshell, would be found in addition to detect vascular edges. Generally, it is unlikely that there are two pixels on the width of a vessel, so the part in  $V$  with the width of two pixels is removed by *SCDVD*. Besides, a vessel is for the most part bar-shaped and not to become a small enclosure, as shown in the red circle of FIGURE 11. Thus, we set a small window with size of  $k \times k$  in *SCDVD*. If vessel pixels in  $V$  form a small enclosure enclosed by the small window, then change these pixels in the enclosure into non-vessel pixels. FIGURE 12 shows the bi-level image  $V$  through the above procedures.

**3. Experiment Result and Discusses.** The purpose of this section is to investigate the performances of our method by experiments. In these experiments, the color images “B1”, “B2”, and “B3” in FIGURE 13 are used as the testing images each of which consists of  $1280 \times 960$  pixels. In these experiments, the variables  $T_l$ ,  $T_h$ ,  $m$ ,  $n$ ,  $THR$ ,  $T_v$ ,  $N$  and  $k$  are by default set to be 0.05, 0.15, 5, 5, 7, 8, 21, and 9. *SCDVD* first takes Canny edge detector to detect the edges in “B1”, “B2”, and “B3”. FIGURE 14 shows the resulted images by applying Canny edge detector to  $B1 \sim B3$ .

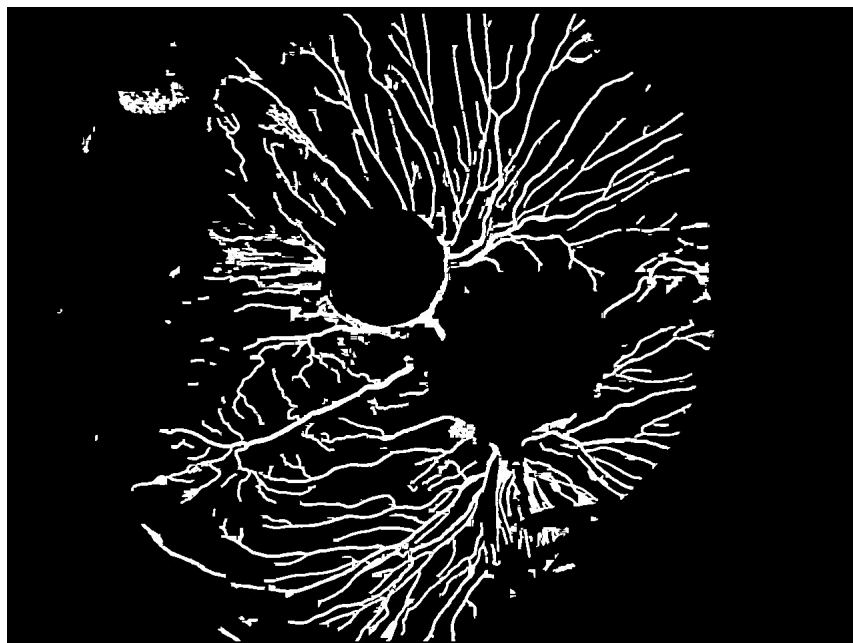


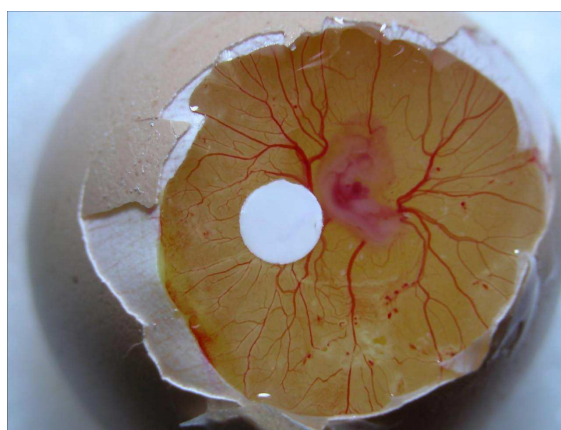
FIGURE 12. The bi-level image  $V$  with removal of eggshell edge and stains



(a)  $B1$



(b)  $B2$



(c)  $B3$

FIGURE 13. Testing images

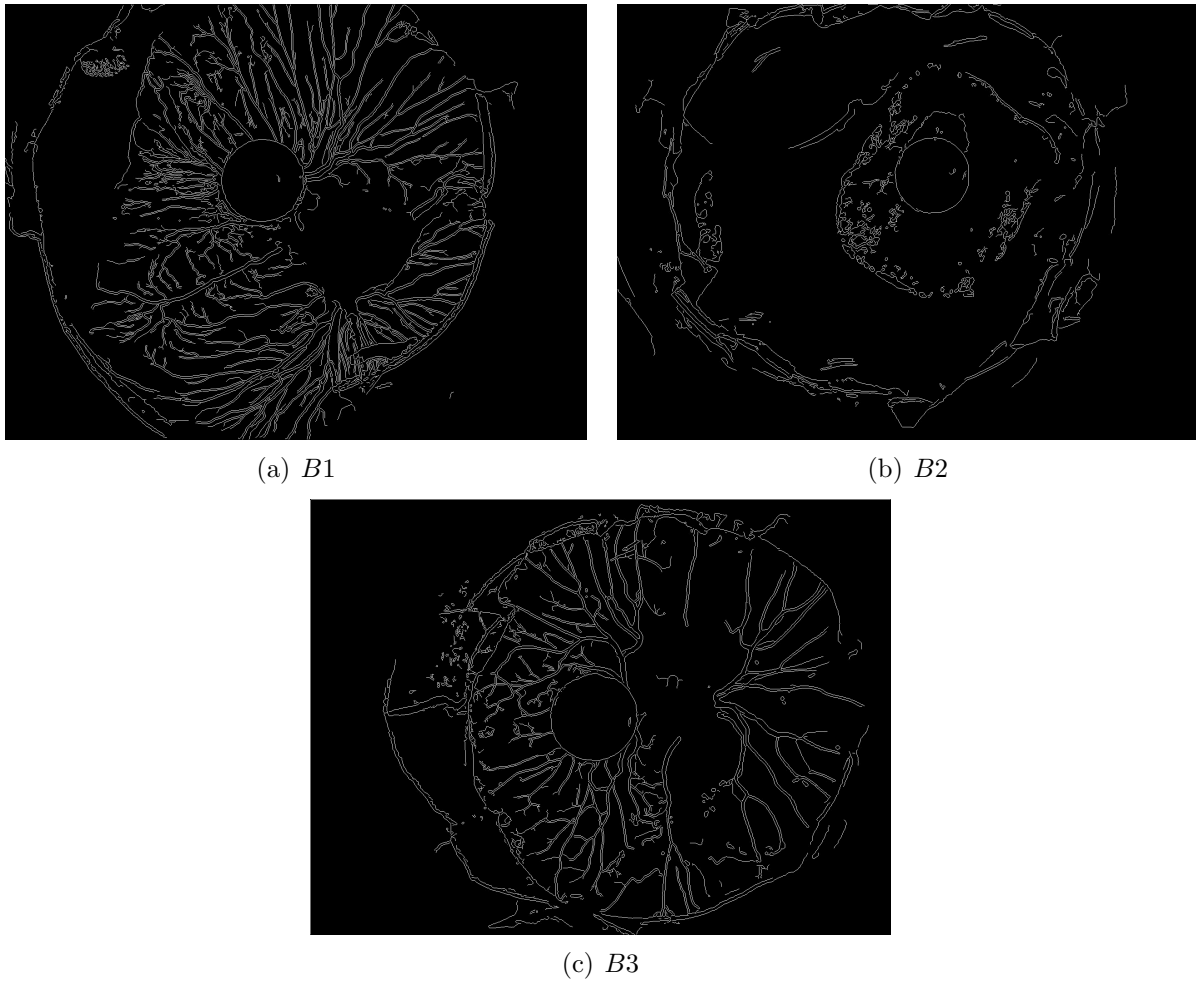


FIGURE 14. The edges on testing images obtained by Canny edge detector

The detected bi-level images are depicted in FIGURE 15 from which we can know most of vessels are found by *SCDVD*, but those tiny capillaries are not discovered and some vessels present the broken phenomenon. Moreover, some non-vessel parts are considered vessels. There are possibly three reasons responsible for the appearances. First, because Canny edge detector uses the gradient changes between pixels to detect edge points, it is unable to find edge points in blood capillaries due to their subtlety in the gradient. Second, noise could happen in an image as a result of photography, scanning, storing, and transferring. The noise would make the color characteristic improper such that the successive steps may detect unsuccessfully vessels to result in the broken phenomenon. Third, Canny edge detector finds not only vascular edges, but also non-vessel edges. If the pixels around these non-vessel edges are considered vessels, a mistake will occur in *SCDVD*.

In spite of some undetected capillaries are undetected, a few detected broken lines or some detected non-vessel parts, i.e. eggshell, calculating *BCD* is to use a fixed  $40 \times 40$  fractal grid put in the center of the checkpoint and then compute the number of grids through which vessels pass, as shown in FIGURE 16. Thus, a few undetected capillaries and a few detected broken lines would not cause too much influence on calculating *BCD*. Furthermore, only a few eggshells could be enclosed by fractal grids, so the error to the correctness of *BCD* is very small. By means of *BCD*, we can analyze the density of vascular distribution. The major objective in the paper is to assist biomedical workers in

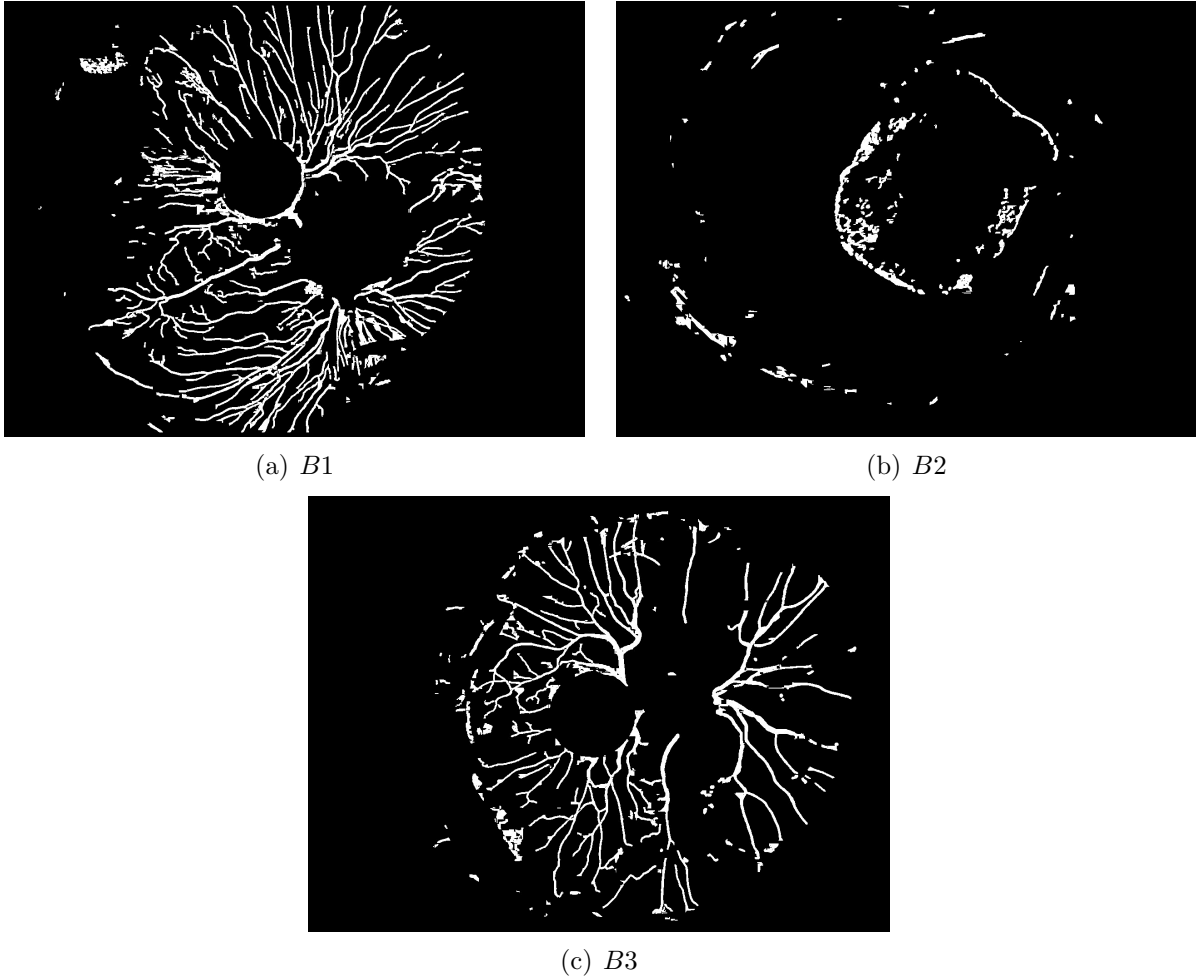


FIGURE 15. The bi-level images detected by *SCDVD*

automatically computing *BCD*. So, our experiments will adopt the *BCD* computed by experts to evaluate the correctness of the *BCD* calculated by *SCDVD*. The calculation way is to put a fixed  $40 \times 40$  fractal grid, where the size of each grid is  $13 \times 13$  pixels, in the center of circle-shaped checkpoint on the chicken chorioallantoic membrane image, as illustrated in FIGURE 16. The definition of *BCD* is stated in Section 1.

In order to prevent a few noises from affect the correctness of calculating *BCD*, *SCDVD* takes advantage of a threshold to determine if there are vessels passing through grids. The threshold value is one tenth of the number of all pixels in a grid. If the number of vessel pixels in the grid is greater than the threshold, then we consider the grid passed by vessels. TABLE 2 presents the *BCD* by experts and that by *SCDVD* in which *Error ratio* is defined as follows:

$$Error\ ratio = \frac{|BCD_E - BCD_{SCDVD}|}{BCD_E}, \quad (5)$$

where  $BCD_E$  and  $BCD_{SCDVD}$  are respectively the *BCD* by experts and that by *SCDVD*. From TABLE 2, we can know the error rations between  $BCD_{SCDVD}$  and  $BCD_E$  are between 2.4% and 3.4%. Thus, it is concluded that *SCDVD* can effectively detect vessels and assist biomedical workers in automatic calculation of *BCD* for the purpose of the follow-up working.

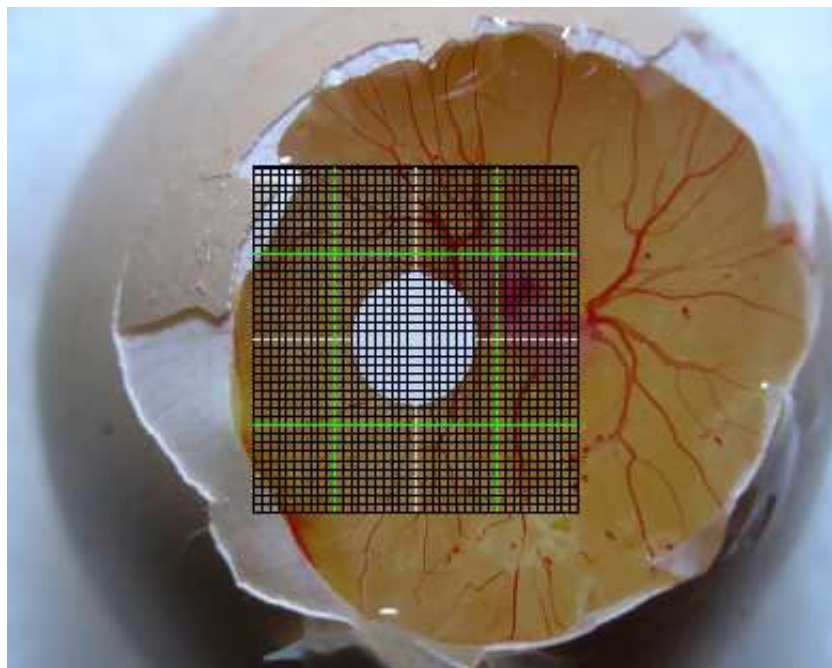


FIGURE 16. Fractal analysis grids

TABLE 2. The  $BCD$  by experts versus that by  $SCDVD$  and their error ratios

Image	$BCD_E$	$BCD_{SCDVD}$	Error ratio (%)
$B1$	1.728	1.776	2.8
$B2$	1.451	1.5	3.4
$B3$	1.68	1.72	2.4

**4. Conclusions.** Production of new blood vessels from original ones is called angiogenesis. Vessel Growth is affected by catalyst and inhibitor, such as Growth factors, Cytokines, Proteolysis enzymes, etc. When the control of angiogenesis loses balance, an abnormal angiogenesis will happen. According to medicine researches, the distribution and density of vascular generation can be used to analyze whether a person suffers from Cancer, Rheumatoid arthritis, Diabetes, Arteriosclerosis or so on. Hence, it is worth studying how to get blood vessel segmentation from the images of organs and further calculate its  $BCD$  in aid of biomedical workers for the follow-up working. In the paper, we propose a method to automatically detect vessels in a chicken chorioallantoic membrane image and compute its  $BCD$ . The first of the approach is to apply Canny edge detector to roughly detect both edges around vessels. Next, we make use of genetic algorithm, with statistics of color distribution and the standard deviation, to find the difference between vessels and others, a characteristic which is further adopted to detect vessels. These detected vessels are finally used to calculate the  $BCD$  of the chicken chorioallantoic membrane image. From experimental results, we see that  $SCDVD$  is able to effectively detect most of vessels and the error ratios between the  $BCD$  by  $SCDVD$  and that by biomedical workers lies between 2.4% to 3.4%.

## REFERENCES

- [1] J. Canny, A computational approach to edge detection, *IEEE Trans., on Pattern Analysis and Machine Intelligence*, vol. 8, no. 6, pp. 679-698, 1986.

- [2] G. Cao, Y. Zhao, and R. Ni, Edge-based blur metric for tamper detection, *Journal of Information Hiding and Multimedia Signal Processing*, vol. 1, no. 1, pp. 20-27, 2010.
- [3] P. Carmeliet, Angiogenesis in life, disease and medicine, *Nature*, vol. 438, no. 7070, pp. 932-936, 2005.
- [4] H. H. Chen, L. L. You, and S. B. Li, Artesunate reduces chicken chorioallantoic membrane neo-vascularisation and exhibits antiangiogenic and apoptotic activity on human microvascular dermal endothelial cell, *Cancer Letters*, vol. 211, no. 2, pp. 163-173, 2004.
- [5] H. Eng, K. Ma, Noise adaptive soft-switching median filter, *IEEE Trans., Image Process*, vol. 10, no. 2, pp. 242-251, 2001.
- [6] J. Folkman, Tumor angiogenesis: therapeutic implications, *New England Journal of Medicine*, vol. 285, no. 21, pp. 1182-1186, 1971.
- [7] J. Folkman, T. Browder, and J. Palmblad, Angiogenesis research: guidelines for translation to clinical application, *Thrombosis and Haemostasis*, vol. 86, no. 1, pp. 23-33, 2001.
- [8] A. J. Hayes, L. Y. Li, and M. E. Lippman, Antivascular therapy: a new approach to cancer treatment, *British Medical Journal*, vol. 318, no. 7187, pp. 853-856, 1999.
- [9] R. Khurana, M. Simmons, J. F. Martin, and I. C. Zachary, Role of angiogenesis in cardiovascular disease: A critical appraisal, *Circulation*, vol.112, no.12, pp.1813-1824, 2005.
- [10] T. Kimura, I. Herzfeld, and G. Valen, Apoptosis and angiogenesis are induced in the unstable atherosclerotic coronary plaque, *Coronary Artery Disease*, vol. 16, no. 3, pp. 191-197, 2005.
- [11] N. Otsu, A threshold selection method form gray-level histograms, *IEEE Trans., of Systems, Man, and Cybernetics*, vol. 9, no. 1, pp. 62-66, 1979.
- [12] L. M. Schmitt, Theory of genetic algorithms, *Theoretical Computer Science*, vol. 259, no. 1-2, pp. 1-61, 2001.
- [13] P. So, E. Barreto, and B. R. Hunt, Box-counting dimension without boxes: Computing D0 from average expansion rates, *Physical Review E*, vol. 60, no. 1, pp. 378-385, 1999.
- [14] B. R. Zetter, Angiogenesis and tumor metastasis, *Annual Review of Medicine*, vol. 49, no. 1407, pp. 407-424, 1998.